Laser-Driven Multiferroics and Ultrafast Spin Current Generation

Masahiro Sato,[1,2,3,4] Shintaro Takayoshi,[5] and Takashi Oka[6,7]

[1]*Department of Physics, Ibaraki University, Mito, Ibaraki 310-8512, Japan*
[2]*Department of Physics and Mathematics, Aoyama-Gakuin University, Sagamihara, Kanagawa 229-8558, Japan*
[3]*Advanced Science Research Center, Japan Atomic Energy Agency, Tokai, Ibaraki 319-1195, Japan*
[4]*ERATO, Japan Science and Technology Agency, Sendai, Miyagi 980-8577, Japan*
[5]*Department of Quantum Matter Physics, University of Geneva, 24 quai Ernest-Ansermet, Geneva 1211, Switzerland*
[6]*Max-Planck-Institut für Physik komplexer Systeme (MPI-PKS), Nöthnitzer Straße 38, Dresden 01187, Germany*
[7]*Max-Planck-Institut für Chemische Physik fester Stoffe (MPI-CPfS), Nöthnitzer Straße 40, Dresden 01187, Germany*

We propose an ultrafast way to generate spin chirality and spin current in a class of multiferroic magnets using a terahertz circularly polarized laser. Using the Floquet formalism for periodically driven systems, we show that it is possible to dynamically control the Dzyaloshinskii-Moriya interaction in materials with magnetoelectric coupling. This is supported by numerical calculations, by which additional resonant phenomena are found. Specifically, when a static magnetic field is applied in addition to the circularly polarized laser, a large resonant enhancement of spin chirality is observed resembling the electron spin resonance. Spin current is generated when the laser is spatially modulated by chiral plasmonic structures and could be detected using optospintronic devices.

Introduction.—Control of emergent collective phenomena by external fields is an important problem in condensed matter. Multiferroic magnets (for a review, see Refs. [1–3]) are opening new possibilities in this direction since the local spins are coupled not only to magnetic fields but to electric fields through the magnetoelectric (ME) coupling. Laser control of materials is attracting interest with a goal of realizing ultrafast and noncontact manipulation [4–14]. In the research community of magnetic systems, control of magnetism using a laser is being studied in the context of spin-pumping and spintronics [4–7]. On the other hand, in the field of electronic systems, periodically driven quantum systems draw the interest of many researchers. When the Hamiltonian is time periodic, the system can be described by the so-called Floquet states [15,16], a temporal analog of the Bloch states, and it is possible to control their quantum nature. For noninteracting systems, the control of the band topology has been studied theoretically [8–10] and experimentally [13,14]. It is possible to understand the effect of a laser through a mapping from the time-dependent Hamiltonian to a *static* effective Hamiltonian using the Floquet theory, and the change of quantum state, e.g., topology and symmetry, is attributed to the emergent terms in the static effective Hamiltonian. This framework can also be applied to quantum magnets. Laser-induced magnetization growth in general quantum magnets [17,18] as well as laser-driven topological spin states [18,19], a quantum spin versions of Floquet topological insulators, were proposed recently.

In the current work, we apply the Floquet theory to quantum *multiferroics* and study the synthetic interactions appearing in the effective Floquet Hamiltonian

[see Eq. (3)]. We show that when elliptically or circularly polarized lasers are applied, an additional Dzyaloshinskii-Moriya (DM) interaction [20] emerges and its direction (DM vector) can be controlled. The DM interaction generally favors a spiral magnetic order and if its strength is spatially modulated, it is possible to induce spin currents. Through direct numerical calculations, we verify this picture, and then propose a way to generate ultrafast spin currents in a realistic device by optical means.

Multiferroics with laser application.—In multiferroics [1–3], spin degrees of freedom couple to electromagnetic waves not only through the Zeeman coupling, but also through the ME coupling. This is because the local polarization vector is related to spin degrees of freedom from crystallographic reasons. The Hamiltonian for multiferroics subject to a laser can be expressed as

$$\mathcal{H}(t) = \mathcal{H}_0 + \mathcal{H}_{\mathrm{E}}(t) + \mathcal{H}_{\mathrm{B}}(t), \tag{1}$$

where $\mathcal{H}_0$ is the spin Hamiltonian, and the laser-driven time-dependent terms $\mathcal{H}_{\mathrm{E}}(t) = -\boldsymbol{E}(t) \cdot \boldsymbol{P}$ and $\mathcal{H}_{\mathrm{B}}(t) = -g\mu_{\mathrm{B}}\boldsymbol{B}(t) \cdot \boldsymbol{S}$, respectively, denote the ME coupling of the total polarization $\boldsymbol{P}$ with electric field $\boldsymbol{E}(t)$, and the Zeeman coupling between the total spin $\boldsymbol{S}$ with the magnetic field $\boldsymbol{B}(t)$ (g is Landé's g factor and μ_{B} is Bohr magneton). The polarization $\boldsymbol{P}$ is given by a function of spin operators. Electric and magnetic components of the laser are represented as $\boldsymbol{E}(t) = E_0\big(\cos(\Omega t + \delta), -\sin(\Omega t), 0\big)$ and $\boldsymbol{B}(t) = E_0 c^{-1}\big(-\sin(\Omega t), -\cos(\Omega t + \delta), 0\big)$, respectively. The value of δ fixes the helicity of the laser, i.e., $\delta = 0$, π, and $\pi/2$, respectively, corresponds to right-circularly, left-circularly, and linearly polarized lasers. Symbols Ω and c

stand for the laser frequency and the speed of light, respectively.

Synthetic interactions from Floquet theory.—We apply the Floquet theory and the Ω^{-1} expansion to Eq. (1). From the discrete Fourier transform of the time-periodic Hamiltonian, $\mathcal{H}(t) = \sum_m e^{-im\Omega t} H_m$ (m: integer), the static effective Hamiltonian $\mathcal{H}_{\text{eff}} = \sum_{i \geq 0} \Omega^{-i} \mathcal{H}_{\text{eff}}^{(i)}$ can be expanded in terms of Ω^{-1} and the leading two terms are given by [21,26,27]

$$\mathcal{H}_{\text{eff}}^{(0)} = H_0, \qquad \mathcal{H}_{\text{eff}}^{(1)} = -\sum_{m>0}[H_{+m}, H_{-m}]/m. \quad (2)$$

For large enough Ω, we can truncate $\mathcal{H}_{\text{eff}}$ up to the Ω^{-1} order. In the present multiferroic system, the first correction $\mathcal{H}_{\text{eff}}^{(1)}$, which we call the synthetic interaction, is given by

$$\mathcal{H}_{\text{syn}} \equiv \Omega^{-1}\mathcal{H}_{\text{eff}}^{(1)} = -\frac{i\cos\delta}{2\Omega}\{\alpha^2[\tilde{P}^x, \tilde{P}^y]$$
$$+ \alpha\beta([\tilde{P}^x, S^x] + [\tilde{P}^y, S^y]) + \beta^2[S^x, S^y]\} \quad (3)$$

with $\alpha = g_{\text{me}}E_0$, and $\beta = g\mu_B E_0 c^{-1}$. Here, g_{me} is the ME coupling constant [see Eq. (4)] with $\tilde{P}$ being a dimensionless function of spins, i.e., $P = g_{\text{me}}\tilde{P}$. Let us comment on the magnitude of the synthetic terms. The strongest magnetic field β of a terahertz (THz) laser attains 1–10 T [28,29]. The magnitude of $g_{\text{me}}(\Omega)$ can be large in a gigahertz (GHz) to THz region [30,31], and from both experimental and theoretical analyses [30–33], the value of α is expected to be of the same order as β. If we use as reference the typical value of exchange coupling $J = 0.1$–10 meV ($\sim$1–100 T) in standard magnets [e.g., *XXZ* magnets in Eq. (7)] both α/J and β/J can achieve values of 0.1–1.

The precise form of the synthetic interaction depends on the type of the ME coupling. Here we consider the case where the polarization $P = \sum_{r,r'} P_{r,r'}$ is given by a product of two spin operators on sites (r, r'). $P_{r,r'}$ is proportional to the exchange interaction (energy density) $S_r \cdot S_{r'}$ in symmetric magnetostriction type multiferroics [34], while it is proportional to the vector spin chirality $S_r \times S_{r'}$ in the antisymmetric magnetostriction type (also known as the inverse DM effect) [32,35–38]. The term $[\tilde{P}^x, \tilde{P}^y]$ thereby yields three spin terms such as the scalar spin chirality. In Ref. [19], it was shown that a three-spin term related to the scalar spin chirality is generated in the symmetric ME coupling case and can induce a topological gap in spin liquids. In addition, $[\tilde{P}^a, S^b]$ and $[S^x, S^y]$ induce two-spin and single-spin terms, respectively.

Two-spin system.—To illustrate the effect of Eq. (3), let us first focus on a simple two-spin multiferroic model depicted in Fig. 1(a). The applied laser travels toward the $-z$ direction, and the two-spin multiferroic magnet is within the xy plane. We assume that the two-spin system
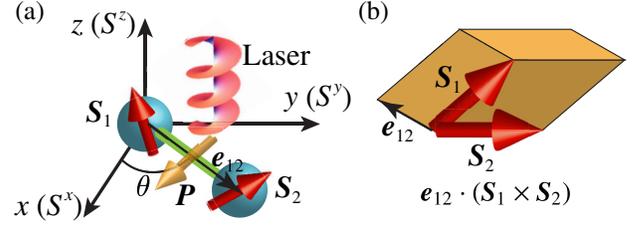

FIG. 1. (a) Schematic picture of a multiferroic system consisting of two spins $S_{1,2}$ in a circularly polarized laser. The vector P represents the electric polarization. (b) Schematic picture for geometric meaning of the synthetic DM interaction in Eq. (5).

$S_{1,2}$ possesses an electric polarization P through the ME coupling as

$$P = g_{\text{me}} e_{12} \times (S_1 \times S_2), \quad (4)$$

where $e_{12} = (\cos\theta, \sin\theta, 0)$ is the vector connecting two spins (the distance between spins is set to unity). This ME coupling is known to be responsible for electric polarization in a wide class of spiral ordered (i.e., chirality ordered) multiferroic magnets [1–3,36–38]. Using Eq. (3), we obtain the synthetic interaction

$$\mathcal{H}_{\text{syn}} = \frac{\alpha\beta}{2\Omega}\cos\delta(e_{12}\cdot\mathcal{V}_{12}) + \frac{\beta^2}{2\Omega}\cos\delta(S_1^z + S_2^z), \quad (5)$$

where $\mathcal{V}_{12} = S_1 \times S_2$ is the vector spin chirality. The first term is the laser-driven DM interaction and generated via the single-photon absorption and emission as shown in Ref. [21]. This DM term is geometrically illustrated by the volume of a parallelepiped as in Fig. 1(b). The three spin term from $[\tilde{P}^x, \tilde{P}^y]$ disappears in Eq. (5) since e_{12} is within the polarization plane.

The result (5) is valid for any spin Hamiltonian $\mathcal{H}_0$ with arbitrary spin magnitude S. In the original model (1), the DM vector in $E(t) \cdot P$ is parallel to z axis. On the other hand, Eq. (5) shows that the synthetic DM vector is in the direction of e_{12}, which is in the xy plane and perpendicular to the z axis. The coefficient $\alpha\beta$ in Eq. (5) indicates that both ME and Zeeman terms are necessary for emergence of the synthetic DM interaction. It is also significant that the laser should be circularly or elliptically polarized. In fact, $\mathcal{H}_{\text{syn}}$ vanishes when the laser is linearly polarized ($\delta = \pi/2$). We emphasize that the synthetic DM coupling constant and its sign can be controlled by changing the laser helicity.

We comment on the importance of breaking the SU(2) symmetry of the system. If the spin Hamiltonian $\mathcal{H}_0$ is spin-rotationally [i.e., SU(2)] symmetric, the Zeeman term $\mathcal{H}_B(t)$ commutes with $\mathcal{H}_0$. This means that the laser-driven β term plays no role in the growth of spin chirality. Thus, it is important that the system has magnetic anisotropy or spontaneous symmetry breakdown that relaxes the SU(2) symmetry.
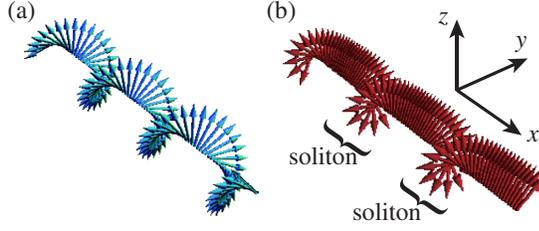
FIG. 2. (a) Spin spiral (helical) ordered state and (b) chiral-soliton-lattice state can be laser-induced if the exchange coupling is AF and FM, respectively.

Many-spin system (spirals and chiral-solitons).—It is straightforward to extend our result (5) to multiferroic magnets consisting of many spins. For instance, the static effective Hamiltonian for an 1D multiferroic spin chain $\mathcal{H}_0^{1D}$ along the x axis ($\theta = 0$) with a circularly polarized laser is given by

$$\mathcal{H}_{\text{eff}}^{1D} = \mathcal{H}_0^{1D} \pm \sum_j \frac{\alpha\beta}{2\Omega} \mathcal{V}_{j,j+1}^x \pm \sum_j \frac{\beta^2}{2\Omega} S_j^z, \quad (6)$$

where $\mathcal{V}_{j,j+1} \equiv \mathbf{S}_j \times \mathbf{S}_{j+1}$, and the sign $\pm$ respectively corresponds to $\delta = 0$ and π. Here we assume that the bond polarization $\mathbf{P}_{j,j+1}$ is proportional to the bond chirality $\mathcal{V}_{j,j+1}$, and the total polarization is given by $\mathbf{P}_{\text{tot}} = g_{\text{me}} \sum_j \mathbf{e}_{j,j+1} \times \mathcal{V}_{j,j+1}$ ($\mathbf{e}_{j,j+1}$ stands for a vector connecting the spin site j and $j+1$).

The effective model (6) is known to support interesting spin states with spatial modulations if the interaction in $\mathcal{H}_0^{1D}$ is short ranged. A spin spiral state [Fig. 2(a)] emerges when the exchange is antiferromagnetic (AF) due to the competition between exchange and laser-induced DM interactions. On the other hand, in the case of a ferromagnetic exchange, it is known that competition among exchange, DM and Zeeman couplings can lead to a chiral-soliton-lattice state [Fig. 2(b)] [39,40] as the classical ground state of $\mathcal{H}_{\text{eff}}^{1D}$. This indicates that a laser can create several types of spiral spin textures depending on lattices and interactions of the multiferroic system $\mathcal{H}_0$.

Numerical analysis.—The Floquet effective Hamiltonian and the predicted emergence of the synthetic interaction (3) are the general result and apply to a broad class of multiferroics. However, there are limitations to the theory: (i) The effective Hamiltonian is applicable when the driving frequency (= photonenergy) Ω is much larger than all the other energy scales in the system, and (ii) when many-body interactions are present, the system eventually heats up [41,42]. As a complementary test, we use a numerical approach and perform direct time dependent calculations in a laser-driven multiferroic model based on $\mathcal{H}(t)$ (1). Here, we focus on simple multiferroic XXZ spin-$\frac{1}{2}$ chains aligned in the x direction ($\theta = 0$) with an external magnetic field H

$$\mathcal{H}_0^{1D} = \mathcal{H}_{XXZ} = \sum_j (J\mathbf{S}_j \cdot \mathbf{S}_{j+1} - J\Delta S_j^x S_{j+1}^x - H S_j^x). \quad (7)$$

In order to break the SU(2) symmetry, we introduced either an Ising anisotropy $-J\Delta S_j^x S_{j+1}^x$ or a static Zeeman term $-HS_j^x$. In the case of circularly polarized laser with $\delta = 0$ ($\delta = \pi$), the effective Hamiltonian Eq. (6) predicts the emergence of x component of vector chirality $\langle \mathcal{V}_{\text{tot}}^x \rangle < 0$ (> 0).

We perform simulations for finite-size systems with L spins. The initial state is set to the ground state of Eq. (7) obtained by numerical diagonalization. The laser is turned on at $t = 0$ and the system evolves according to the time-dependent Hamiltonian $\mathcal{H}(t)$ (1). The time evolution of the state $|\Psi(t)\rangle$ is obtained by integrating the Schrödinger equation $i(d/dt)|\Psi(t)\rangle = \mathcal{H}(t)|\Psi(t)\rangle$ using the fifth order Runge-Kutta method. In the numerical analysis below, we set $\alpha/J = \beta/J = 0.2$.

First, consider the case of $\Delta = 0.5$ and $H = 0$. In Figs. 3(a) and 3(b), we plot the typical time evolutions of vector chirality $\langle \mathcal{V}_{\text{tot}}(t) \rangle = \langle \sum_j \mathcal{V}_{j,j+1}(t) \rangle$ and magnetization $\mathbf{M}_{\text{tot}}(t) = \langle \sum_j \mathbf{S}_j(t) \rangle$ for an XXZ model with $H = 0$ in a circularly polarized laser with $\Omega/J = 2$ and $\delta = 0$. The vector chirality $\langle \mathcal{V}_{\text{tot}}^x(t) \rangle < 0$ appears as expected while $\langle \mathcal{V}_{\text{tot}}^{(y,z)}(t) \rangle$ remains small. The dependence of the vector chirality on the laser helicity δ is depicted in Figs. 3(c) and 3(d). We see that $\langle \mathcal{V}_{\text{tot}}^x(t) \rangle$ becomes negative (positive) for $\delta = 0$ (π), while it remains very small for linear polarization $\delta = \pi/2$. These behaviors are consistent with the prediction (6) from the Floquet theory. However, the vector chirality does not keep on growing but becomes saturated around $t/J^{-1} \sim 400$ in Fig. 3(c). This may be due to heating; the system's "effective temperature" exceeds the magnitude of
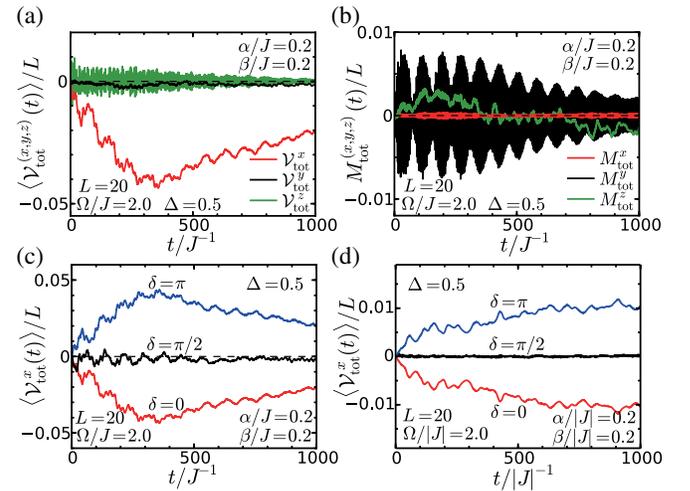

FIG. 3. Simulation results of a multiferroic XXZ chain ($\Delta = 0.5$, $H/J = 0$) in a circularly polarized laser. Time evolutions of (a) vector chirality $\langle \mathcal{V}_{\text{tot}}(t) \rangle$ and (b) magnetization $\mathbf{M}_{\text{tot}}(t)$ in an AF XXZ model under a circularly polarized laser ($J > 0$ and $\delta = 0$). (c) Laser helicity (δ) dependence of $\langle \mathcal{V}_{\text{tot}}^x(t) \rangle$. (d) Time evolution of vector chirality in the case of a ferromagnetic exchange ($J < 0$).
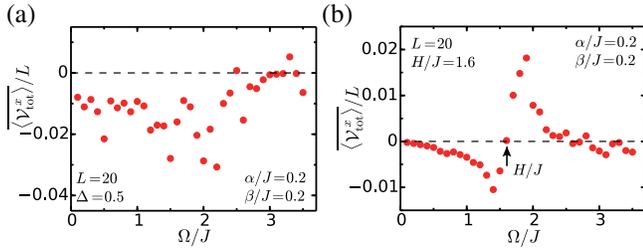
FIG. 4. Ω dependence of time average of vector chirality $\overline{\langle \mathcal{V}^x_{\text{tot}} \rangle}$ in (a) AF ($J > 0$) XXZ model without external magnetic field and (b) Heisenberg model ($\Delta = 0$) with external magnetic field. Around $\Omega = H$, we observe a large magnitude of laser-driven chirality due to a resonant behavior.
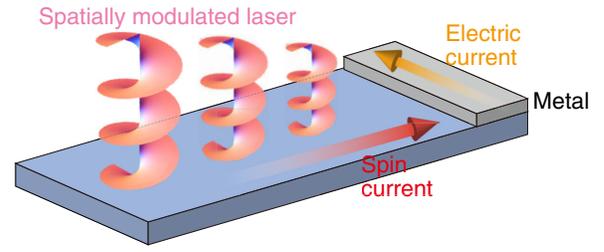

FIG. 5. Setup to detect signatures of laser-driven DM interactions by measuring spin current. The spin current pumped from a spin chain to a metal with a strong spin-orbit coupling is changed into an electric current via inverse spin Hall effect in the metal.

the synthetic term ($\sim \alpha\beta/\Omega$) around this time, and the linear growth of the chirality stops. This is consistent with recent studies on "heating" in closed periodically driven systems that have revealed that the effective Hamiltonian approach, e.g., Eq. (6), is valid only for finite time, and if the driving is continued the system will approach an infinite temperature state [41,42]. When the system is coupled to a heat reservoir, the heating can be stopped and the system can be stabilized [12]. Figure 3(b) shows that the magnetization $M_{\text{tot}}(t)$ does not grow but only exhibits an oscillation with small amplitude.

In order to understand how the induced chirality depends on the laser frequency Ω, we define its time average as

$$\overline{\langle \mathcal{V}_{\text{tot}} \rangle} \equiv \frac{1}{T} \int_0^T dt \langle \mathcal{V}_{\text{tot}}(t) \rangle \qquad (8)$$

with $T = 1000 \, J^{-1}$. As shown in Fig. 4(a), for the XXZ chain in zero field, the induced chirality is typically negative, which agrees with the prediction from the Floquet effective Hamiltonian (6), but since Eq. (6) is based on the high frequency expansion, it fails to explain the detailed structure in the simulation. We find many small peaks in Fig. 4(a) that are presumably due to resonance with many-body excited states.

We also consider laser-driven spin chains in a static magnetic field. Naively, we may expect that the magnetic field will play the same role as the Ising anisotropy, i.e., a source to break the SU(2) symmetry, and no qualitative difference would occur. However, in Fig. 4(b), the result of direct calculation shows a resonant behavior in the generation of a vector chirality around $\Omega \sim H$, which is clearly not described by the effective Hamiltonian (6). We verified that a similar resonant behavior also occurs in a multiferroic spin-1 chain and a spin-$\frac{1}{2}$ ladder (see Supplemental Material [21]), which indicates that the resonance around $\Omega \sim H$ is universal in a broad class of multiferroic systems. What happens around $\Omega \sim H$ is analogous to electron spin resonance (ESR). Thus, our calculation implies that by using a circularly polarized laser in an ESR setup, it is possible to efficiently generate a vector chirality in multiferroics.

Detection schemes.—Finally, we propose schemes to detect the synthetic DM interaction and vector chirality. Detection using pump-probe optical methods is in principle possible by observing nontrivial textures, e.g., spiral states [21]. Another scheme is to utilize optospintronic methods with plasmon resonances proposed in Ref. [43]. The underling idea is to apply a *spatially modulated* circularly polarized laser to a multiferroic magnet (Fig. 5). Assuming that the exchange coupling is dominant in the time-dependent Hamiltonian of the spin chain $\mathcal{H}_{XXZ} + \mathcal{H}_{\text{E}}(t) + \mathcal{H}_{\text{B}}(t)$, the Heisenberg equation of motion shows that

$$i(dS^x_j/dt) \approx [S^x_j, \mathcal{H}_{XXZ}] = iJ(\mathcal{V}^x_{j-1,j} - \mathcal{V}^x_{j,j+1}). \qquad (9)$$

Similar expressions hold for higher dimensions and therefore a finite spin current $\langle dS^x_j/dt \rangle$ appears due to a site-dependent vector chirality if the laser is spatially modulated. A circularly polarized laser with large spatial modulation can be realized in the near field of chiral plasmonic structures [44]. Then, in order to detect the spin current, one needs to combine the plasmonic structure with a metallic electrode where the spin current is transformed into an electric current by inverse spin Hall effect [45–48]. The spin current is injected from the multiferroic magnet to the electrode if $\langle dS^x_j/dt \rangle$ is nonzero at the interface [49,50]. Using materials with strong spin-orbit coupling such as Pt [48] for the electrode, we can observe the generation of a laser-driven chirality through an electric voltage drop. In the Supplemental Material [21], we numerically show that an inhomogeneous chirality appears when we apply a spatially modulated laser.

Distinction of mechanisms is an important issue. In contrast with other effects of laser such as heating, the laser-driven DM interaction strongly depends on the direction of the laser as can be seen from Fig. 1 and Eq. (4), and thus systematic measurements with sample rotation are useful for making clear the origin.

Summary.—In conclusion, we proposed a way to generate and control DM interactions and spin currents in multiferroics utilizing elliptically polarized lasers. Our

understanding is based on the Floquet theory with the Ω^{-1} expansion, which captures the general tendency of the numerical results, while we find an additional resonant enhancement of spin chirality when a static magnetic field is applied.

[1] Y. Tokura, S. Seki, and N. Nagaosa, Rep. Prog. Phys. **77,** 076501 (2014).
[2] Y. Tokura and S. Seki, Adv. Mater. **22,** 1554 (2010).
[3] K. F. Wang, J.-M. Liu, and Z. F. Ren, Adv. Phys. **58,** 321 (2009).
[4] A. Kirilyuk, A. V. Kimel, and T. Rasing, Rev. Mod. Phys. **82,** 2731 (2010).
[5] C. Vicario, C. Ruchert, F. Ardana-Lamas, P. M. Derlet, B. Tudu, J. Luning, and C. P. Hauri, Nat. Photonics **7,** 720 (2013).
[6] A. J. Schellekens, K. C. Kuiper, R. R. J. C. de Wit, and B. Koopmans, Nat. Commun. **5,** 4333 (2014).
[7] G. Choi, B. Min, K. Lee, and D. G. Cahill, Nat. Commun. **5,** 4334 (2014).
[8] T. Oka and H. Aoki, Phys. Rev. B **79,** 081406(R) (2009).
[9] T. Kitagawa, T. Oka, A. Brataas, L. Fu, and E. Demler, Phys. Rev. B **84,** 235108 (2011).
[10] N. H. Lindner, G. Refael, and V. Galitski, Nat. Phys. **7,** 490 (2011).
[11] N. Tsuji, T. Oka, and H. Aoki, Phys. Rev. B **78,** 235124 (2008).
[12] N. Tsuji, T. Oka, and H. Aoki, Phys. Rev. Lett. **103,** 047403 (2009).
[13] Y. H. Wang, H. Steinberg, P. Jarillo-Herrero, and N. Gedik, Science **342,** 453 (2013).
[14] G. Jotzu, M. Messer, Rémi Desbuquois, M. Lebrat, T. Uehlinger, D. Greif, and T. Esslinger, Nature (London) **515,** 237 (2014).
[15] J. H. Shirley, Phys. Rev. **138,** B979 (1965).
[16] H. Sambe, Phys. Rev. A **7,** 2203 (1973).
[17] S. Takayoshi, H. Aoki, and T. Oka, Phys. Rev. B **90,** 085150 (2014).
[18] S. Takayoshi, M. Sato, and T. Oka, Phys. Rev. B **90,** 214413 (2014).
[19] M. Sato, Y. Sasaki, and T. Oka, arXiv:1404.2010.
[20] I. Dzyaloshinsky, J. Phys. Chem. Solids **4,** 241 (1958); T. Moriya, Phys. Rev. **120,** 91 (1960).
[21] See Supplemental Material at http://link.aps.org/supplemental/10.1103/PhysRevLett.117.147202, which includes Refs. [9,22–25], for the details of our theoretical methods, our additional numerical results, and proposed experimental ways.
[22] C. Kittel, *Introduction to Solid State Physics* (Wiley, New York, 2004).
[23] T. Mikami, S. Kitamura, K. Yasuda, N. Tsuji, T. Oka, and H. Aoki, Phys. Rev. B **93,** 144307 (2016).
[24] S. Miyahara and N. Furukawa, J. Phys. Soc. Jpn. **81,** 023712 (2012).
[25] S. Kibayashi, Y. Takahashi, S. Seki, and Y. Tokura, Nat. Commun. **5,** 4583 (2014).
[26] F. Casas, J. A. Oteo, and J. Ros, J. Phys. A **34,** 3379 (2001).
[27] E. S. Mananga and T. Charpentier, J. Chem. Phys. **135,** 044109 (2011).
[28] H. Hirori, K. Shinokita, M. Shirai, S. Tani, Y. Kadoya, and K. Tanaka, Nat. Commun. **2,** 594 (2011).
[29] A. Pashkin, F. Junginger, B. Mayer, C. Schmidt, O. Schubert, D. Brida, R. Huber, and A. Leitenstorfer, IEEE J. Sel. Topics Quant. Electr. **19,** 8401608 (2013).
[30] Y. Takahashi, R. Shimano, Y. Kaneko, H. Murakawa, and Y. Tokura, Nat. Phys. **8,** 121 (2012).
[31] D. Hüvonen, U. Nagel, T. Rõõm, Y. J. Choi, C. L. Zhang, S. Park, and S.-W. Cheong, Phys. Rev. B **80,** 100402(R) (2009).
[32] H. Katsura, A. V. Balatsky, and N. Nagaosa, Phys. Rev. Lett. **98,** 027203 (2007).
[33] S. Furukawa, M. Sato, and S. Onoda, Phys. Rev. Lett. **105,** 257205 (2010).
[34] T. Moriya, J. Phys. Soc. Jpn. **23,** 490 (1967); J. Appl. Phys. **39,** 1042 (1968).
[35] Y. Tanabe, T. Moriya, and S. Sugano, Phys. Rev. Lett. **15,** 1023 (1965).
[36] H. Katsura, N. Nagaosa, and A. V. Balatsky, Phys. Rev. Lett. **95,** 057205 (2005).
[37] M. Mostovoy, Phys. Rev. Lett. **96,** 067601 (2006).
[38] I. A. Sergienko and E. Dagotto, Phys. Rev. B **73,** 094434 (2006).
[39] J. Kishine, K. Inoue, and Y. Yoshida, Prog. Theor. Phys. Suppl. **159,** 82 (2005).
[40] Y. Togawa, Y. Kousaka, S. Nishihara, K. Inoue, J. Akimitsu, A. S. Ovchinnikov, and J. Kishine, Phys. Rev. Lett. **111,** 197204 (2013).
[41] L. D'Alessio and M. Rigol, Phys. Rev. X **4,** 041048 (2014).
[42] A. Lazarides, A. Das, and R. Moessner, Phys. Rev. E **90,** 012110 (2014).
[43] K. Uchida, H. Adachi, T. Kikkawa, S. Ito, Z. Qiu, S. Maekawa, and E. Saitoh, Nat. Commun. **6,** 5910 (2015).
[44] M. Schäferling, D. Dregely, M. Hentschel, and H. Giessen, Phys. Rev. X **2,** 031010 (2012).
[45] E. Saitoh, M. Ueda, H. Miyajima, and G. Tatara, Appl. Phys. Lett. **88,** 182509 (2006).
[46] S. O. Valenzuela and M. Tinkham, Nature (London) **442,** 176 (2006).
[47] *Spin Current*, edited by S. Maekawa, S. O. Valenzuela, E. Saitoh, and T. Kimura (Oxford University Press, Oxford, England, 2012).
[48] K. Uchida, H. Adachi, T. Kikkawa, A. Kirihara, M. Ishida, S. Yorozu, S. Maekawa, and E. Saitoh, Proc. IEEE **104,** 1946 (2016).
[49] Y. Tserkovnyak, A. Brataas, and G. E. W. Bauer, Phys. Rev. Lett. **88,** 117601 (2002).
[50] H. Adachi, K. Uchida, E. Saitoh, and S. Maekawa, Rep. Prog. Phys. **76,** 036501 (2013).